Phys. Status Solidi RRL **6**, No. 5, 226–228 (2012) / **DOI** 10.1002/pssr.201206064

pss +++rapid research letters+++
www.pss-rapid.com

Crystal recovery from Al-implantation induced damaging in 3C-SiC films

Andrea Severino[*,1,2], **Nicolò Piluso**[1,2], **Antonio Marino**[2], **and Francesco La Via**[2]

[1] Epitaxial Technology Center, ETC srl, 16° strada, Blocco Torre Allegra, 95121 Catania, Italy
[2] CNR-IMM, Sezione di Catania, VIII Strada, 95121 Catania, Italy

Received 13 February 2012, revised 13 April 2012, accepted 13 April 2012
Published online 18 April 2012

Keywords p-type implanted 3C-SiC, reciprocal space mapping, high-temperature annealing, crystal recovery

[*] Corresponding author: e-mail andrea.severino@imm.cnr.it, Phone: +0039 095 5968322, Fax: +0039 095 5968312

Damaging in Al-implanted 3C-SiC and subsequent crystal recovery due to thermal treatments up to 1350 °C are evaluated by X-ray diffraction and micro-Raman spectroscopy. Reciprocal space mapping of (004) 3C-SiC planes shows a low-intensity implantation-induced secondary peak at higher interplanar spacing in the as-implanted 3C-SiC sample, with a generated misfit between the implanted and the epitaxial region of about 0.6%. Increasing the annealing temperature from 950 °C to 1350 °C, the secondary peak is gradually reabsorbed within the epitaxial 3C-SiC reciprocal lattice point. Finally, the disappearance of the secondary peak after a 1350 °C thermal treatment is observed. Thus, implantation-induced average strain, resulting in a severe 3C-SiC deformation, has been totally relieved at the highest annealing temperature.

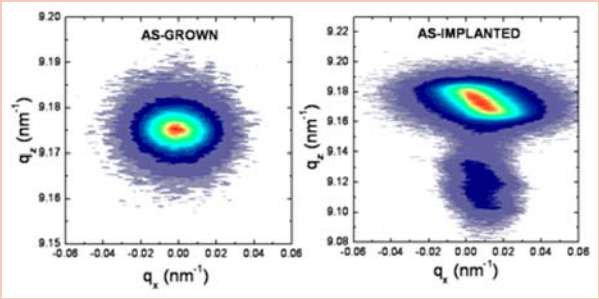

3C-SiC is considered an attractive material for power electronics devices due to its excellent properties such as higher theoretical electron mobility (~900 $cm^2 V^{-1} s^{-1}$) and lower interface state density between SiC and SiO_2 when compared to the most technological mature 4H-SiC polytype. Both these properties make 3C-SiC very attractive for metal–oxide–semiconductor field effect transistors (MOSFETs) working in medium- and high-power regimes [1]. Moreover, single crystal 3C-SiC is grown at a lower temperature than 4H-SiC and heteroepitaxy with large-area Si substrates is allowed, thus reducing drastically the cost for its production [2]. The epitaxy of doped 3C-SiC films is easily achievable by using gaseous dopants during the growth process with nitrogen and aluminium as most used doping species [3, 4]. A much harder step is the definition of localized doping region underneath the drain and/or source for MOSFET realization. The most used technique to obtain such structures is to implant N, Al or B ions in the desired regions [5, 6]. For p-type doping, Al is preferred due to its shallow energetic levels and, consequently, lower activation energy (0.24 eV). Ion implantation processing, on the other hand, involves the scattering of the ordered atoms in SiC lattice with high-energetic ions (from tenth to thousands keV) resulting in a damaging of the crystal structure of the hosting material.

In this study, a 10 μm thick 3C-SiC film has been processed to realize an Al^+-implanted layer underneath the film surface. The structural damaging and recovery due to the implantation processing and subsequent thermal annealing have been evaluated by means of X-ray diffraction (XRD) and micro-Raman spectroscopy (μ-Raman). Reciprocal space mapping (RSM) of the (004) 3C-SiC reciprocal lattice point (RLP) was then used to further study the recovery at different temperatures.

3C-SiC was grown in a chemical vapor deposition (CVD) reactor by using a multi-step growth process [7]. 3C-SiC growth process was performed on a (001)-oriented Si substrate by using ethylene (C_2H_4), trichlorosilane

(TCS) and hydrogen (H_2). After the carbonization step, performed during the temperature ramp up from 1100 °C to 1370 °C in C_2H_4 ambient, the growth proceeded at a growth rate of 3 μm/h. 3C-SiC film was unintentionally n-type doped (~5×10^{15} cm^{-3}). This wafer was processed within TANDETRON accelerator to realize the p-type region in 3C-SiC by heating up the target to 400 °C to minimize the amorphization of SiC, observed at room temperature [8]. The Al^+ ions were accelerated at four different energies of 40 keV, 170 keV, 350 keV and 700 keV with four ion doses of 4×10^{14} cm^{-2}, 4×10^{13} cm^{-2}, 7×10^{13} cm^{-2}, 1×10^{14} cm^{-2}, respectively. The profile of the implant is obtained by SRIM simulation, at Al^+ ion doses and energies used on a target material with the mass density of 3C-SiC (3.22 g/cm^3). The final profile gives an implantation depth of about 1 μm in the film with a uniform Al^+ ion concentration of 2×10^{18} at/cm^3. The implanted wafer was then cut into four pieces (2×4 cm^2) and each sample was annealed at temperatures from 950 °C to 1350 °C within CVD reactor in Ar for 60 minutes. Ion implantation process affects the crystal order of any target material, the disorder depending on several parameters such as ion dose, energy and temperature. Annealing processes are required to recover the crystal structure from implantation damaging and for doping activation. The structural order can be recovered once the energy of re-organization of atoms in the lattice is achieved.

In order to evaluate the recovery from implantation damaging, XRD and μ-Raman measurements were performed. A Bruker AXS D8 discover diffractometer with a Cu K_{α_1} X-ray source (wavelength $\lambda = 1.54062$ Å) and a (022) four-bounce Ge monochromator at primary beam has been used. X-ray rocking curves have been performed on a spatial map over 25 points for each sample thanks to a high-precision goniometer and a motorized stage. Raman spectra have been collected using a HR800 integrated system by Horiba Jobin–Yvon in a backscattering configuration. The excitation wavelength was 325 nm, supplied by a He–Cd laser. In Fig. 1, full widths at half maximum (FWHM) of (004) 3C-SiC rocking curves (ω-scans) for all samples are reported on the left axis while, on the right axis, intensity ratios (I_{TO}/I_{LO}) of the transverse optical (TO) over longitudinal optical (LO) 3C-SiC Raman mode are displayed. These two parameters are excellent gauges to study the crystal quality. Looking at Fig. 1, it is possible to observe a reduction of FWHM values increasing the annealing temperature. In detail, the FWHM of the implanted sample is higher than that of the as-grown and, after the thermal treatments, FWHM values decrease. The trend observed in Fig. 1 is further confirmed by micro-Raman spectroscopy. In a (100) cubic material with a high density of planar faults, such as 3C-SiC on Si, the TO mode, forbidden by selection rules, is often observed. This ratio is very close to zero for the as-grown sample while it jumps up to a value of 5.57 in the as-implanted sample. In annealed samples, a strong reduction of the I_{TO}/I_{LO} ratio with increasing annealing temperature is observed with a similar

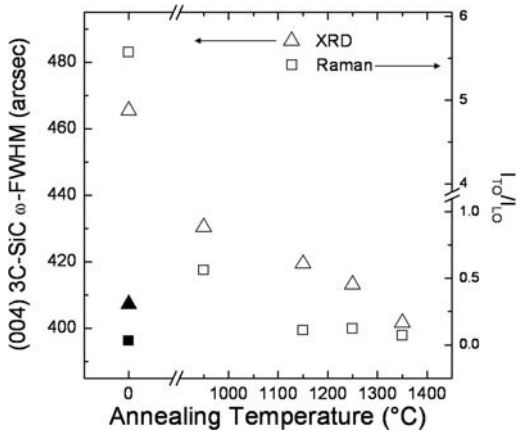

Figure 1 Values of (004) 3C-SiC ω-FWHM and I_{TO}/I_{LO} intensity ratio with annealing temperature. Full and open symbols refer to the as-grown and processed material, respectively.

trend shown in Fig. 1. Thus, both XRD and Raman spectroscopy suggest an improvement of the crystal quality, indicating an effective recovery from implantation-induced damage.

To confirm the recovery of the crystal structure with the annealing temperature, the (004) 3C-SiC reciprocal lattice point (RLP) of 3C-SiC has been studied. The (004) 3C-SiC RLP was evaluated by performing RSM with $2\theta-\omega$ scans repeated with a variation in the ω offset for each scan. RSM has been used in literature to evaluate average (macro-)strain and lattice disorder due to ion implantation in other materials [9]. In Fig. 2, (004) 3C-SiC RSM of the as-grown sample (a), as-implanted sample (b), annealed at 950 °C (c), and annealed at 1350 °C (d), respectively, are displayed. In Fig. 2b, it can be noted a low-intensity secondary peak at lower 2θ, i.e. higher $d_{(004)}$ interplanar spacing ($d_{sec} = 1.09658$ Å), close to the high-intensity epitaxial peak ($d_{epi} = 1.09002$ Å). Moreover, the epitaxial SiC peak shows a very large broadening indicating a large variation of the interplanar spacing in 3C-SiC. This effect is not observed in the as-grown material ($d_{epi} = 1.08990$ Å), where the broadening is limited, indicating a reduced residual macro-strain due to the heteroepitaxial growth process. These two maps suggest that the implantation process is resulting in a large damaging, with a high degree of mosaicity and macro-strain in the implanted film. The second peak, very low in intensity due to the limited volume of the implanted region, may be addressed to a deformation of the 3C-SiC lattice, resulting in an expanded Al^+-implanted 3C-SiC cell. In detail, the value f_{IMP} of the induced misfit due to the implantation process of Al^+ ions can be determined from Eq. (1), giving a value of about 6.02×10^{-3} (0.6%).

$$f_{IMP} = \frac{|d_{epi} - d_{sec}|}{d_{epi}}. \quad (1)$$

When the 950 °C-annealed sample is considered, a shoulder very close to the epitaxial peak is still observed.

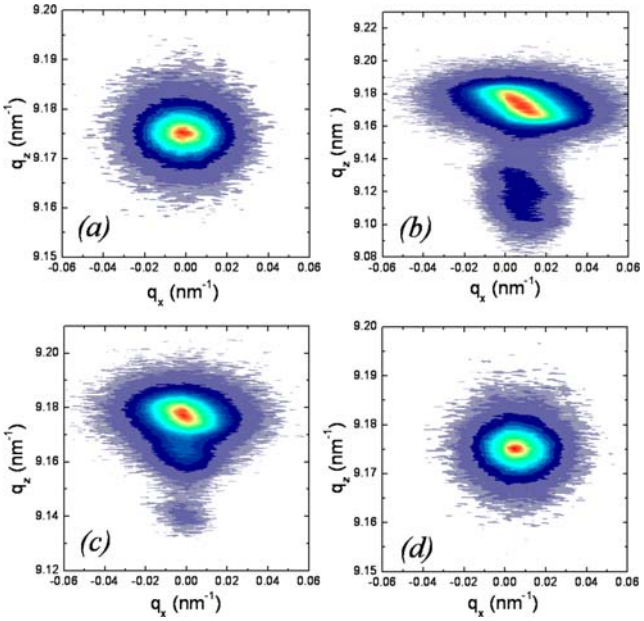

Figure 2 (online colour at: www.pss-rapid.com) (004) Reciprocal space mappings of as-grown 3C-SiC film (a), as-implanted film (b), annealed at 950 °C (c), and annealed at 1350 °C (d), respectively. In (b), a second low-intensity peak can be observed at lower q_z (i.e. higher d_{004}). This peak becomes a shoulder of the main epitaxial peak in (c).

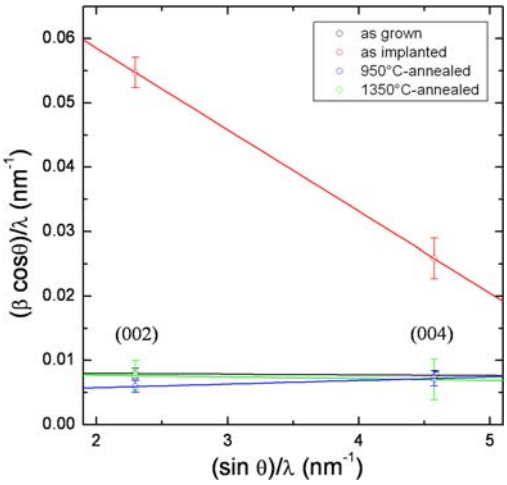

Figure 3 (online colour at: www.pss-rapid.com) Williamson–Hall plots of as-grown sample (black), as-implanted (red), 950 °C annealed sample (blue) and 1350 °C annealed sample (green) extracted from $2\theta-\omega$ line profile broadening of symmetric (002) and (004) 3C-SiC reflections.

Here, the crystal recovery is taking place, indicating that the lattice deformation is partially reabsorbed thanks to the thermal process occurred. Finally, in 1350 °C annealed sample, an almost complete 3C-SiC crystal recovery is observed, with the absence of any extra peak in the map (d_{epi} = 1.08986 Å).

The change in the lattice deformation suggests a change in the microstructure from the as-grown material to the annealed sample. Microstrain and size broadenings of a line profile are usually studied plotting a Williamson–Hall plot, as shown in Fig. 3, with a linear dependency when an important contribution of microstrain broadening is involved. In this work, pseudo-Voigt functions were found to better fit the experimental $2\theta-\omega$ profiles of symmetric 3C-SiC reflections. As suggested by Srikant et al., the resultant broadening should be the sum of the starting distributions (Gaussian and Cauchy), weighed by the Lorentz content of the resultant distribution [10]. A simple comparison between inclinations of the lines shows an important difference of the as-implanted sample (very steep slope) with other samples reported (almost flat). We speculate that the deformation of the 3C-SiC lattice induced by Al-implantation is affecting drastically the microstructure of the target material (3C-SiC) leading to severe distortion of the microstructure. When the as-implanted sample is annealed, the macro-strain is eventually recovered and, as a consequence, the microstructure is rearranged reducing the microstrain. Indeed, Williamson–Hall plots of annealed samples show up as almost constant lines, typical of materials where the broadening is mainly due to size components (due to defects such as antiphase boundaries).

The observation of an almost complete recovery of the crystal structure at 1350 °C is, however, in contrast with what observed in some previous study on implanted 3C-SiC [8, 9]. A possible explanation can be due to the relatively low ion concentration used in this work, which facilitates the crystal recovery.

In this Letter, we have reported on Al^+ ion implantation in 3C-SiC. XRD and Raman spectroscopy indicate an excellent recovery of the 3C-SiC crystal structure after thermal treatment at 1350 °C. Reciprocal space mappings and Williamson–Hall plots show that the lattice deformation induced by the implantation is gradually reabsorbed as the annealing temperature is increased.

References

[1] H. Nagasawa et al., Phys. Status Solidi B **245**, 1272 (2008).
[2] A. Severino et al., Thin Solid Films **518**, S165 (2010).
[3] M. Zielinski et al., J. Cryst. Growth **310**, 3174 (2008).
[4] L. Wang et al., J. Cryst. Growth **329**, 67 (2011).
[5] X. Song et al., Nucl. Instrum. Methods Phys. Res. B **269**, 2020 (2011).
[6] M. V. Rao et al., J. Appl. Phys. **77**, 2479 (1995).
[7] A. Severino and F. La Via, Appl. Phys. Lett. **97**, 181916 (2010).
[8] H. Itoh et al., J. Appl. Phys. **82**, 5339 (1997).
[9] E. Abramof et al., Nucl. Instrum. Methods Phys. Res. **175–177**, 229 (2001).
[10] V. Srikant et al., J. Appl. Phys. **82**, 4286 (1997).

